

## Introduction to special section: Coastal Advances in Shelf Transport

J. A. Barth and P. A. Wheeler

College of Oceanic and Atmospheric Sciences, Oregon State University, Corvallis, Oregon, USA

Received 24 June 2005; accepted 25 July 2005; published 25 October 2005.

[1] The Coastal Ocean Advances in Shelf Transport (COAST) program conducted an interdisciplinary study of coastal upwelling off central Oregon during summer 2001. Two intensive field efforts during May–June and August 2001 were coordinated with ocean circulation, ecosystem, and atmospheric modeling of the region. A primary goal was to contrast the coastal ocean response to wind forcing in a region of relatively simple alongshore bottom topography versus that associated with a substantial submarine bank. In this overview we provide background motivation for the COAST project and summarize the major research findings.

**Citation:** Barth, J. A., and P. A. Wheeler (2005), Introduction to special section: Coastal Advances in Shelf Transport, *J. Geophys. Res.*, 110, C10S01, doi:10.1029/2005JC003124.

### 1. Introduction and Background

[2] Wind-driven coastal upwelling in regions with relatively uniform alongshore bottom topography and a straight coastline has been extensively studied. For example, off central Oregon the mean wind forcing is southward during summer (upwelling favorable), becoming so after a spring transition [Huyer *et al.*, 1979]. The southward wind drives an offshore surface Ekman layer flux which is balanced by upwelling of subsurface water near the coast. Isopycnals rise to the ocean surface and form a front between recently upwelled, cold, nutrient-rich water inshore and oceanic water offshore [Halpern, 1976; Mooers *et al.*, 1976]. The upwelling front moves offshore with continued wind forcing and is often found near the midshelf. Accompanying the strong cross-shelf density gradient across the front is a vertically sheared, southward upwelling jet [Mooers *et al.*, 1976]. Off central Oregon, the core of the upwelling jet is found at mid shelf (80–100 m water depth) with summertime average near-surface speed of  $0.35 \text{ m s}^{-1}$  and velocities in individual events in excess of  $0.8 \text{ m s}^{-1}$  [Huyer *et al.*, 1978]. Variations in the alongshelf flow are correlated for long distances ( $\sim 80 \text{ km}$ ) in the alongshore direction [Kundu and Allen, 1976]. The observed offshore surface transport is roughly equal to the theoretical wind-driven Ekman transport if account is taken for the wind-driven momentum penetrating below the surface mixed layer [Lentz, 1992]. For a typical 20 knot southward alongshore wind, the offshore Ekman transport distributed over a 30-m-deep layer results in a  $0.06 \text{ m s}^{-1}$  flow. The compensatory onshore flow off Oregon is found primarily in the interior of the water column [Smith, 1981] as can be inferred because large Burger number flows (i.e., strong stratification) tend to suppress transport in the bottom boundary layer [Lentz and Chapman, 2004].

[3] The coastal ocean off Oregon is strongly wind driven, so any investigation of the coastal ecosystem in that region must start with a fundamental understanding of the wind forcing. Perlin *et al.* [2004] use measurements from the SeaWinds scatterometer on NASA's Quick Scatterometer (QuikSCAT) and meteorological buoys, and output from several atmospheric models to characterize the surface wind stress field off Oregon and northern California during the summers (June–September) of 2000 and 2001. For the Heceta Bank region in central Oregon they find mean southward wind stress of  $0.05 \text{ N m}^{-2}$  ( $\sim 10$  knot wind speed), consistent with previous studies in this region [e.g., Samelson *et al.*, 2002]. Both Perlin *et al.* [2004] and Samelson *et al.* [2002] find a southward increase of the southward mean wind stress along central Oregon, but little mean wind stress curl in the offshore region, relative to that associated with the orographically modified flow south of Cape Blanco, OR ( $43^\circ\text{N}$ ). These studies also demonstrated that the summer mean diurnal cycle of wind stress at NDBC buoy 46050 off Newport (Figure 1) has an amplitude of about  $0.02 \text{ N m}^{-2}$ , with maximum southward alongshore wind stress in the evening.

[4] In most of the COAST study region, tidal currents from individual tidal constituents (e.g., M2, K1) are expected to be about  $0.05 \text{ m s}^{-1}$ , smaller than the subtidal, wind-driven alongshelf flows. Using an array of current meters extending across the Oregon continental slope and shelf, Torgrimson and Hickey [1979] reported M2 (K1) semimajor axis amplitudes of  $0.02$ – $0.06$  ( $0.02$ – $0.04$ )  $\text{m s}^{-1}$ . Using a data-assimilating model together with high-frequency coastal radar and moored acoustic Doppler profiler velocities, Erofeeva *et al.* [2003] find similar magnitudes for the M2 and K1 currents except in a region directly over Heceta Bank where K1 velocities reach  $0.10 \text{ m s}^{-1}$  through a resonance of the tide with a first-mode barotropic shelf wave. The baroclinic tide is challenging to estimate and highly variable in time and space, as it depends upon the density structure in the water column. Semidiurnal (M2) baroclinic tidal currents at the

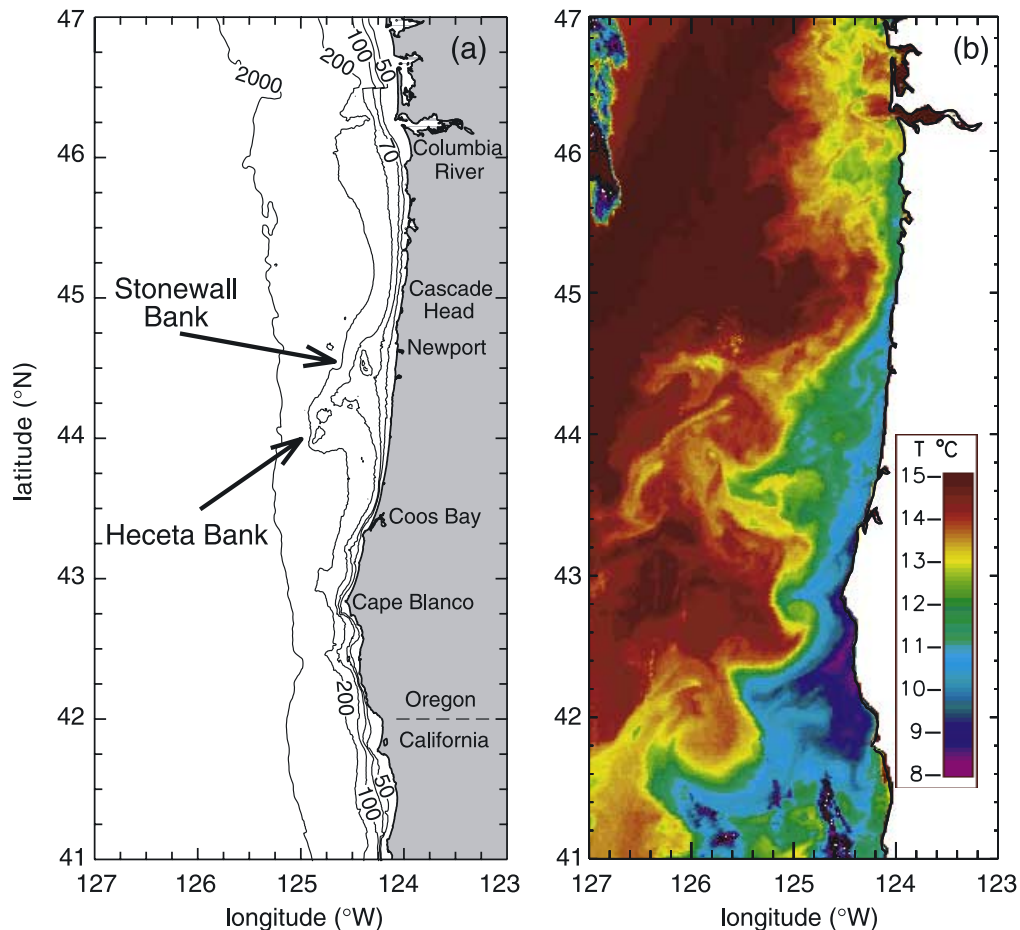


**Figure 1.** (a) Oregon coastal region with bottom topography in meters showing the location of Heceta and Stonewall Banks. Isobaths in meters. (b) Satellite sea surface temperature image from 13 August 1995.

surface off Oregon can be as large as  $0.10 \text{ m s}^{-1}$  [Torgripson and Hickey, 1979; Kurapov *et al.*, 2003].

[5] Cross-shelf distributions of nutrients, phytoplankton and zooplankton during summer upwelling off central Oregon have been previously studied by Wroblewski [1977], Peterson *et al.* [1979], and Small and Menzies [1981]. More recent results show similar patterns and are described here. Mean surface nitrate concentrations during the upwelling season range from 2 to  $30 \mu\text{M}$  over the inner and midshelf [Corwith and Wheeler, 2002]. Offshore surface nitrate concentrations are depleted to less than  $0.1 \mu\text{M}$  within about 50 km of the coast, but with some extension of higher nitrate concentrations beyond Heceta Bank [Hill and Wheeler, 2002]. Usually nitrate goes to depletion in surface water when significant levels of phosphate and silicate are still present [Corwith and Wheeler, 2002]. In the region around Cape Blanco in August, surface concentrations of  $\text{pCO}_2$ , phosphate and silicate vary between 150 and  $690 \mu\text{atm}$ , 0.1 and 1.8, and 1 and  $33 \mu\text{M}$ , respectively [van Geen *et al.*, 2000].

[6] In general, chlorophyll is very low ( $<0.1 \text{ mg m}^{-3}$ ) in oceanic waters, and high to moderate ( $1\text{--}10 \text{ mg m}^{-3}$ ) in shelf and slope waters. Highest surface chlorophyll concentrations are found in the inshore zone out to the 100 m isobath [Small and Menzies, 1981]. Prior to 1999, the

distribution of trace metals, including iron, had not been directly studied off Oregon, but has been of renewed interest given the suggestion of Hutchins and Bruland [1998] that coastal phytoplankton may be limited by micronutrient inputs, especially iron. Chase *et al.* [2002] show that surface water iron and nitrogen concentrations were highly variable and uncoupled, and that the primary sources of iron to Oregon coastal waters were from shelf or slope sediments and the Columbia River. From their measurements, they conclude that the distribution of phytoplankton appeared to be driven primarily by physical dynamics and was not linked to the distribution of iron. Nevertheless, Chase *et al.* [2002] did find evidence that cross-shelf nutrient distributions and phytoplankton fluorescence characteristics were consistent with iron regulation of phytoplankton physiology in some areas. An important unanswered question from these studies is the relative degree to which the availability of macro- and micronutrients or the effects of the physical flow field contribute to produce the observed cross-shelf distributions and cross-shelf transport of nutrients and chlorophyll.

[7] Off the coast of Newport the zooplankton are dominated by subarctic species including *Calanus marshallae*, *Pseudocalanus mimus*, *Acartia hudsonica* and *A. longiremis* with highest standing stocks on the shelf. Copepod biomass

in shelf waters is higher by a factor of 3–5 than that observed in slope waters [Morgan *et al.*, 2003; Keister and Peterson, 2003]. Cross-shelf zonation is observed in their distributions as well as with *Acartia hudsonica* almost completely restricted to waters within 5 km of the coast, whereas *Pseudocalanus mimus* and *A. longiremis* are found primarily in mid- to outer-shelf regions. *Calanus marshallae* eggs and larvae are found chiefly in inner- to midshelf waters whereas older juveniles and adults are found in outer-shelf waters [Peterson *et al.*, 1979]. The unique cross-shelf distribution of copepod biomass, and of the species *A. hudsonica* and *C. marshallae* were modeled by Wroblewski [1977, 1980, 1982]. Euphausiids are also important and the two dominant species exhibit distinct onshore-offshore distribution patterns. *Thysanoessa spinifera* is almost always restricted to the shelf while *Euphausia pacifica* resides chiefly in slope waters [Smiles and Percy, 1970; Feinberg and Peterson, 2003]. It is clear from these studies that there are distinct upwelling zones versus offshore communities of phytoplankton and zooplankton. What remains to be determined are the physical, chemical and biological features that regulate the community composition and distributions in these coastal waters.

[8] The presence of alongshore topographic variations on otherwise relatively straight continental shelves has a profound influence on coastal circulation and hence the local ecosystem. Examples of alongshore topographic features include changes in bottom topography with or without changes in coastline orientation, e.g., submarine canyons [Hickey, 1997] and banks [Butman *et al.*, 1982], and coastal promontories with or without changes in the bathymetry directly offshore [e.g., Barth *et al.*, 2000]. Topographic features may disrupt or redirect strong alongshore coastal jets, create regions of weaker flow in their “shadow” and lead to enhanced mixing.

[9] In this overview, we report the results of recent field work off central Oregon to determine the influence of Heceta and Stonewall Banks on the coastal upwelling system. The Heceta Bank complex (we will refer to the Heceta and Stonewall Banks region as the bank “complex” or simply the “Bank”) rises to over 50% of the surrounding water column depth on the continental shelf off central Oregon (44°20'N) (Figure 1). The Banks extend about 100 km in the alongshelf direction and widen the shelf to 60 km from the relatively narrow 25-km-wide shelves both to the north and south of the Bank. Stonewall Bank rises to within 7 m of the ocean surface and the offshore pinnacles of Heceta Bank are 46 m deep at their shallowest. A commercially important fishery is associated with Heceta Bank [Percy *et al.*, 1989] and cold, chlorophyll-rich upwelled water has been observed well seaward of the continental shelf break south of the Bank [Barth *et al.*, 2000, 2005b; Hill and Wheeler, 2002].

[10] Recent renewed interest in the Heceta Bank region has been motivated by its role in influencing the distributions of juvenile salmonids, sea birds and cetaceans relative to physical oceanographic fields (temperature, salinity, velocity) and distributions of phyto- and zooplankton [Batchelder *et al.*, 2002]. The appearance of hypoxic bottom waters over the inshore side of the Heceta Bank complex in 2002 and the subsequent die-offs of fish and

invertebrates has also drawn attention to this region [Grantham *et al.*, 2004].

## 2. Coastal Ocean Advances in Shelf Transport (COAST) Program

[11] Two intensive field efforts were conducted as part of the Coastal Ocean Advances in Shelf Transport (COAST) project in summer 2001 together with coordinated ocean circulation, ecosystem and atmospheric modeling. A primary goal was to contrast the coastal ocean response to wind forcing in a region of relatively simple alongshore bottom topography versus that associated with a substantial submarine bank. A second objective was to determine how the hydrographic and velocity structure influences the magnitude and distribution of primary and secondary production in this region.

[12] During May–June and August 2001, two vessels conducted interdisciplinary research off central Oregon (Figure 2). One ship conducted rapid, high-spatial-resolution surveys of the three-dimensional thermohaline, velocity and bio-optical fields using a towed, undulating vehicle and shipboard ADCP (region bounded by thick solid line in Figure 2). Surface maps of nutrients and iron were also made. A second ship collected high-vertical-resolution cross-shelf profiles along 44.25 and 45°N (dashed E-W lines in Figure 2) of water properties: temperature, salinity and turbulence parameters from a loosely tethered microstructure profiler; nutrients, carbonate species, phytoplankton photosynthetic parameters, and particulate and dissolved organic material from a pumped profiling system. An instrumented aircraft measured properties of the lower atmosphere and upper ocean during and between the month-long intensive field experiments. A set of moorings measured physical, bio-optical and meteorological parameters from May to August 2001 [Boyd *et al.*, 2002], and a land-based radio system continuously measured surface currents hourly over a region encompassing much of the COAST study region (Figure 2). A high-resolution, three-dimensional shelf circulation and coupled ecosystem ocean model, and a mesoscale atmospheric model were used to investigate the dynamics of the system.

## 3. Overview of Findings

### 3.1. Wind Forcing

[13] Bane *et al.* [2005] use in situ and aircraft observations to analyze the meteorological conditions during the summer 2001 COAST experiment and characterize wind conditions during both southward and northward winds. In summary, when both mean and diurnal components are included, the greatest (least) alongshore stress occurs near sunset for southward (northward) winds, and least (greatest) alongshore stress in the morning for southward (northward) winds. New results include the observation of semidiurnal fluctuations in surface air temperature, apparently forced by nonlinear internal ocean tides, and of a stable internal boundary layer within the marine atmospheric boundary layer. This internal boundary layer formed over cool upwelled waters, had surface air temperatures 1°C lower near the coast than offshore, and had somewhat reduced wind stress. An additional new result is the recognition of the existence of

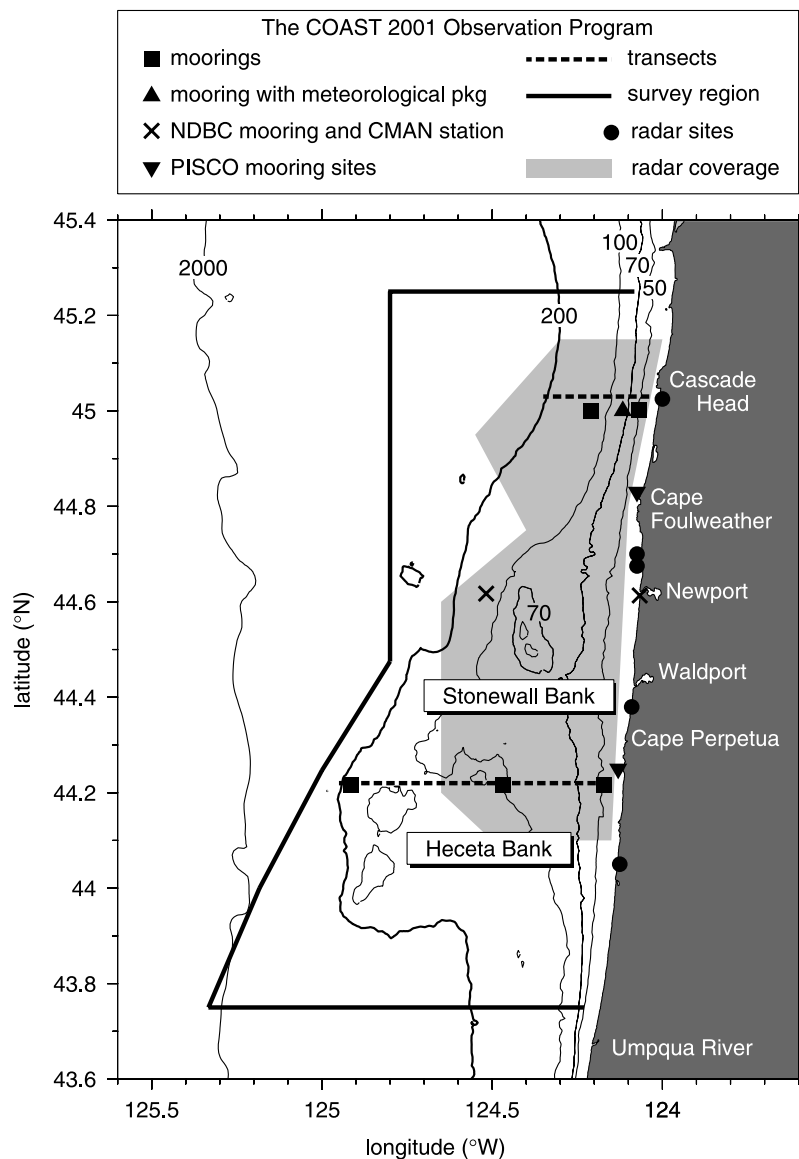


**Figure 2.** Coastal Ocean Advances in Shelf Transport (COAST) summer 2001 ocean and atmosphere observation program. The large survey region was sampled by both an oceanographic vessel and an aircraft. The east-west transect along 45.01°N has been moved 2.4 km north for clarity. Isobaths in meters.

alongshore wind stress oscillations with periods near 20 days, which were found to correlate with north-south position changes in the jet stream at the same periodicities. These intraseasonal stress oscillations drove 20-day oscillations in upper ocean temperature, which had amplitudes near 4°C.

### 3.2. Wind-Driven Circulation

[14] In a study using 17 deployments of bottom-mounted acoustic Doppler current profilers during the summer upwelling seasons of 1999 and 2001–2003 as part of the Partnership for Interdisciplinary Studies of Coastal Oceans (PISCO) program, *Kirincich et al.* [2005] demonstrate that the measured surface and bottom cross-shelf Ekman transports in 15 m of water at 1–2 km offshore were 25% of full theoretical Ekman transport based on the observed wind

stress. Measured transports reached full Ekman transport 5–6 km offshore in 50 m of water. A weak linear relationship was found between water column stratification and the fraction of full Ekman transport, with reduced cross-shelf transport during times of decreased stratification. *Kirincich et al.* [2005] point out the potential for significant impacts on the inner-shelf ecosystem from this “shutdown” of cross-shelf circulation, e.g., sequestering production in the nearshore and reducing larval cross-shelf transport.

[15] While much of the research off central Oregon during summer has focused on upwelling conditions, *Barth et al.* [2005a] and *Kosro* [2005] report the coastal ocean response to a strong summertime downwelling event during August 2001. Northward wind stress of up to 0.25 N m<sup>-2</sup> (30 knot winds) lasting 3–4 days resulted in onshore surface Ekman transport, northward near-surface currents

of  $0.2\text{--}0.3\text{ m s}^{-1}$  and the formation of a downwelling front intersecting the bottom at about the 40 m isobath. Vigorous wind-driven mixing, with vertical overturning scales of up to 15 m estimated using a microstructure instrument on-board a towed undulating vehicle [Ott *et al.*, 2003, 2004], leads to a nearshore region of low buoyancy frequency above the downwelled pycnocline. The downwelling circulation also transports organic matter from the euphotic zone to the sea floor over the inner continental shelf [Barth *et al.*, 2005a].

### 3.3. Flow-Topography Interaction: Observations

[16] One of the main goals of the COAST program was to investigate the coastal upwelling circulation and ecosystem response in the Heceta Bank region where there is considerable alongshore bottom bathymetry variation (Figure 1). Indications that flow-topography interactions occur in this region are apparent in satellite SST imagery [e.g., Barth *et al.*, 2000], but the region had not been studied in detail before the Global Ocean Ecosystem Dynamics (GLOBEC) 2000 and COAST 2001 field experiments. Barth *et al.* [2000], in a study of the coastal jet separation process near Cape Blanco, suggested that an offshore excursion of upwelled water occurred as the southward flowing upwelling jet interacted with Heceta Bank. They estimated that about half a Sverdrup (Sv) ( $10^6\text{ m}^3\text{ s}^{-1}$ ) of water (estimated from integrating the geostrophic current from 0 to 200 m) flowed offshore off the southern end of Heceta Bank in August. While the GLOBEC field effort documented the influence of physical circulation on the distribution of organisms over Heceta Bank, spatial and temporal resolution was limited because GLOBEC required observations over a much larger region from Newport, Oregon, to Crescent City, California [Batchelder *et al.*, 2002].

[17] A detailed study covering a few square kilometers over Stonewall Bank ( $44.5^\circ\text{N}$ ) (Figure 1) revealed intense mixing as flow interacted with the submarine bank [Moum and Nash, 2000]. Turbulent diffusivities over the bank were 100 times greater than estimates on the shelf away from bottom topographic variations. The total drag exerted by the bank on the flow was a combination of bottom friction and form drag, and was of sufficient size to decelerate the flow over the bank in a few hours.

[18] During the COAST summer 2001 experiment, repeated high-resolution hydrographic and velocity surveys were conducted over Heceta Bank using a towed, undulating vehicle and shipboard ADCP [Castelao and Barth, 2005, hereinafter referred to as CB; Barth *et al.*, 2005a, hereinafter referred to as BPC]. Upwelling over simple topography north of Heceta Bank ( $45^\circ\text{N}$ ) (Figure 1) exhibited a classic response with a midshelf (80–100 m), baroclinic coastal jet and upwelled isopycnals. The upper water column was influenced by both upwelling and fresh water from the Columbia River [Barnes *et al.*, 1972]. The coastal upwelling jet followed the midshelf isobaths to the southwest around Heceta Bank. The equatorward jet is located inshore of the pinnacles of the Bank ( $124.8^\circ\text{--}124.9^\circ\text{W}$ ,  $44.0^\circ\text{--}44.2^\circ\text{N}$ ) (Figure 1) during spring, but moves over and seaward of the pinnacles late in the upwelling season (August) (CB). The region influenced by upwelling is much broader during summer, both north of and over Heceta Bank (CB), a result also apparent in

surveys from summer 2000 [Barth *et al.*, 2005b]. At the southern end of the Bank, where the shelfbreak turns almost  $90^\circ$  back toward the coast, the coastal upwelling jet separates from the continental shelf and transports about 0.7 and 0.4 Sv off the shelf during spring and summer, respectively (CB).

[19] The region inshore on Heceta Bank, i.e., inshore of the separating coastal upwelling jet, is characterized by low velocities (CB; BPC) [Kosro, 2005]. Northward flow is often observed on the inshore part of southern Heceta Bank arising from cyclonic motion of the flow as it adjusts to a deepening water column at the southern end of the Bank (CB; BPC). Strong northward flow is also found inshore on Heceta Bank in response to both wind relaxation and strong downwelling favorable winds (BPC) [Kosro, 2005]. By creating an east-west perturbation in the coastal upwelling front, the flow-topography interaction introduces an along-shore pressure gradient that can drive flow to the north during wind relaxation. The combination of northward flows inshore on the Bank and the southwestward flowing coastal upwelling jet on the outer Bank, can lead to complete recirculation of water parcels around the Bank on a timescale of about 10 days (BPC).

[20] The low-velocity region inshore on the Bank was also found to have high ( $> 15\text{ mg m}^{-3}$ ) near-surface values of chlorophyll, presumably the result of favorable conditions for phytoplankton growth outweighing advective loss in this region (BPC). This high primary productivity forms the basis for success at higher trophic levels [Batchelder *et al.*, 2002; Lamb and Peterson, 2005]. On the other hand, increased primary productivity over the Bank, sinking of that material to the bottom, and its subsequent respiration by microbial activity can lead to the formation of hypoxic bottom waters in that region [Grantham *et al.*, 2004]. A low-temperature, high-salinity bottom water pool was found over the inshore side of the Bank. This bottom pool is up to 40 m thick and contains elevated levels of suspended material. Dense water in this pool is influenced by water from the north early in the upwelling season, but its primary source is from the south (CB).

[21] More details of the time-varying surface circulation in the COAST region were obtained using hourly surface current maps made during April–September 2001 using five land-based, high-frequency radar systems (Figure 2) [Kosro, 2005]. This data set shows that the surface currents responded rapidly to the changing winds and exhibited spatial patterns strongly influenced by bottom topography. The orientation, strength and offshore location of the wind-driven coastal upwelling jet changed near Cape Foulweather ( $44.8^\circ\text{N}$ ) (Figure 1), with the core of the equatorward jet following the 80 m isobath between  $45^\circ$  and  $44.4^\circ\text{N}$ . Currents inshore of the jet were generally weak, but a second equatorward jet was observed on the southern, inshore part of Heceta Bank (near Waldport,  $44.4^\circ\text{N}$ ). Downwelling winds produced strongest poleward flow near the coast. Surface currents were correlated with the north-south wind, responding within half a day, except far from shore over Heceta Bank indicating the flow is less coupled to the wind in that region. By using the unique radar-derived spatial time series of surface currents, Kosro [2005] showed that the wind-driven response varied spatially, i.e., was intensified in the narrow, straight-shelf northern region,

and that the equatorward jet persisted through periods of zero wind forcing.

#### 3.4. Flow-Topography Interaction: Modeling

[22] Extensive modeling of the circulation in the central Oregon region was conducted as part of the COAST project and its predecessors, in particular the National Oceanographic Partnership Program “Prediction of Wind-Driven Coastal Circulation (1998–2000)” project. Using a periodic channel model extending from  $43^{\circ}$  to  $46^{\circ}$ N forced by observed winds and surface heat flux, *Oke et al.* [2002b, 2002c] found that the circulation north of Heceta Bank is well described by classical upwelling theory. They also found that the coastal upwelling jet is deflected around Heceta Bank and the flow features they describe for southern Heceta Bank (an equatorward jet offshore near the Heceta Bank pinnacles and a second nearshore coastal upwelling jet, between which is found weak or reversed flow) compare well with those detailed by the COAST observational program. *Oke et al.* [2002c] used the model to show that the deep upwelled water inshore of the Heceta Bank pinnacles is drawn from the south during mid-July 1999 and is sometimes not connected with deep water to the north, in agreement with in situ observations presented in CB. Lastly, they used the numerical model to demonstrate that inshore of the coastal jet the acceleration of the alongshore flow is small and is driven by the difference between the surface stress and a negative alongshore pressure gradient. During wind relaxation, negative pressure gradients drive northward flow inshore on Heceta Bank.

[23] *Gan and Allen* [2005] extend the studies of *Oke et al.* [2002b, 2002c] by modeling a larger domain ( $41.7^{\circ}$ – $47.3^{\circ}$ N) and using observed winds and surface heat fluxes from the COAST summer 2001 meteorological buoy to drive the model. Their results were similar to those of *Oke et al.* [2002b, 2002c] including deflection of the coastal upwelling jet around Heceta Bank, a cyclonic turning of the jet as it transited the southern end of the Bank, and negative pressure gradients driving northward flow inshore of the coastal upwelling jet during wind relaxation, all of which are seen in the COAST observational data. *Gan and Allen* [2005] also use detailed momentum and heat budgets as a function of depth and horizontal location to demonstrate the different balances between north of and over Heceta Bank, for example the added importance of alongshore advection in the balancing heat inshore over the Bank.

#### 3.5. Bottom Boundary Layer Processes

[24] Closely spaced vertical profiles through the entire water column from the sea surface to the sea floor and moored measurements were used by COAST investigators to reveal details of the bottom boundary layer hydrographic, velocity and turbulent structure. Most of these results are from the region with relatively simple alongshore bathymetry ( $45^{\circ}$ N) (Figure 1). *Perlin et al.* [2005a] show that well-mixed and turbulent bottom boundary layers were typically less than 10 m high, but exceeded 20 m during relaxation from upwelling consistent with existing theories of stratified flow over a sloping bottom [e.g., *Trowbridge and Lentz*, 1991]. *Moum et al.* [2004] show that the increased bottom boundary layer thickness during relaxation from upwelling is consistent with convectively driven mixing as a result of

lighter fluid forced beneath heavier fluid by downslope bottom Ekman layer transport. The vertical structure of properties near the bottom versus nondimensional depth is similar to those near the ocean surface during convection. *Moum et al.* [2004] found that the greater the buoyancy anomaly is near the bottom, the greater the turbulent dissipation rate in the neutral layer away from the bottom.

[25] The measured profiles of bottom boundary layer properties motivated *Perlin et al.* [2005b] to propose a modified law-of-the-wall velocity profile near the bottom which accounts for stratification. While the velocity profile right near the bottom (the lower 20% of the mixed bottom boundary layer) agrees well with classical law-of-the-wall scaling, farther from the bottom horizontal velocities decrease faster with height than predicted using a single turbulent mixing length. *Perlin et al.* [2005b] introduce a new turbulent mixing length scale to account for suppression of velocity fluctuations by stratification in the upper part of the boundary layer and their resulting predictions of velocity profiles agree well with observations. The modified law-of-the-wall gives a new scaling for turbulent dissipation rate which diverges from classical predictions above the lower 20% of the bottom boundary layer and agrees with direct observations of dissipation rate and velocity profiles up to 60% of the boundary layer height.

[26] *Perlin et al.* [2005a] track the intersection of near-bottom isopycnals with the bottom through a sequence of upwelling and relaxation events to estimate the cross-shelf speed in the bottom boundary layer. The cross-shelf speed (up to  $7 \text{ km d}^{-1}$  onshelf during upwelling, and up to  $5 \text{ km d}^{-1}$  offshelf during relaxation) agrees well with estimates from bottom Ekman layer theory using an estimate of the bottom friction velocity derived from bottom stress measurements. These measurements confirm that Ekman balance of alongshore momentum in the bottom boundary layer holds across the full shelf width rather than just at discrete locations as shown previously [e.g., *Trowbridge and Lentz*, 1998].

[27] Motivated by differences in bottom mixed layer height at different locations within the COAST region apparent in a numerical circulation model, *Kurapov et al.* [2005c] show the importance of curl-driven upwelling near the bottom driven by the overlying currents. At  $45^{\circ}$ N, the bottom mixed layer grows in response to downwelling favorable conditions, in agreement with existing theories [e.g., *Trowbridge and Lentz*, 1991], but farther to the south the bottom mixed layer increases following upwelling events. *Kurapov et al.* [2005c] show that this increased bottom mixed layer height (in excess of 20 m, comparable to maximum values at  $45^{\circ}$ N during downwelling) may be attributed to curl-driven upwelling caused by horizontal gradients of alongshelf velocity on the inshore side of the separated coastal upwelling jet. An indication of thicker bottom mixed layers during upwelling over the Heceta Bank region inshore of the separated coastal upwelling jet is provided by near-bottom observations from a towed, undulating vehicle presented by *Barth et al.* [2005a].

#### 3.6. Data Assimilation

[28] *Kurapov et al.* [2005a, 2005b] use a numerical circulation model that assimilates currents from moorings deployed as part of COAST during summer 2001. The data

assimilation technique is based on an optimal interpolation sequential algorithm using a stationary estimate of the forecast error covariance obtained from the error covariance in the model solution not constrained by data assimilation. The data assimilation techniques build on previous work of *Oke et al.* [2002a] who assimilated surface velocities obtained from land-based coastal radar arrays. Assimilation of currents from one or two of the COAST 2001 moorings located on the path of the upwelling jet helps to improve the model-data error and correlation at locations up to 90 km north or south from the assimilation sites [*Kurapov et al.*, 2005a]. Improvement to the south from assimilation in the north occurs because the coastal jet is flowing southward, and improvement in the north from assimilation in the south presumably occurs because this is the direction for coastal trapped wave propagation. Predictions are not improved if mooring data from the shadow zone inshore of the separated coastal upwelling jet are assimilated. In *Kurapov et al.* [2005b], the analysis is extended to include comparisons between model predictions and surface velocities from land-based coastal radar; sea surface height at the coast; hydrographic data from SeaSoar observations and near-bottom turbulence parameters. They demonstrate that significant improvement is achieved for the nearshore sea surface height and for the slopes of the isopycnals (i.e., horizontal density gradients) on the southern flank of Heceta Bank when moored velocities from just a few current meter moorings were assimilated. *Kurapov et al.* [2005b] further demonstrate that assimilating both moored velocity and salinity data improves the transport of buoyant surface water as influenced by Columbia River in the COAST region.

### 3.7. Biogeochemistry

[29] Wind driven upwelling of nutrients to the surface water in coastal regions has often been depicted as a two-dimensional “conveyor belt” system with transport of high-nutrient water into the euphotic zone by advection [*Dugdale and Wilkerson*, 1989]. *Hales et al.* [2005] update this concept by using a unique combination of high-spatial-resolution measurements of vertical nutrient gradients and turbulent fluxes to compare the reversible exchange of nutrients during upwelling and downwelling events with the cross-isopycnal turbulent vertical fluxes. The wind-driven upwelling circulation moves the bottom boundary layer in the onshore direction while a reduction or reversal of the alongshore winds leads to a downwelling circulation that moves the bottom boundary layer back offshore [*Lentz*, 1992; *Perlin et al.*, 2005a], i.e., a reversible upwelling/downwelling advection along isopycnal surfaces. The other main contribution to upwelled nutrients is an irreversible turbulent mixing that transports nutrients upward across isopycnal surfaces. *Hales et al.* [2005] estimate that this irreversible flux of nitrate due to turbulent mixing, the majority of which occurs shoreward of the 75 m isobath, accounts for 25% of the total nutrient supply in the euphotic zone.

[30] *Hales et al.* [2004] describe the first-ever high-resolution, cross-shelf vertical sections of carbonate chemistry in the upper 200 m of the water column off the Oregon coast. Surface values from these measurements agree well with earlier high-resolution mapping near Cape Blanco [*van*

*Geen et al.*, 2000]. The cross-shelf vertical sections show the effects of strong upwelling of CO<sub>2</sub>-rich water followed by rapid biological uptake [*Hales et al.*, 2004]. As nitrate and CO<sub>2</sub> are taken up by phytoplankton, the P<sub>CO2</sub> concentrations fall below atmospheric saturation and the surface water off the coast becomes a strong sink for atmospheric CO<sub>2</sub> during the summer upwelling season. This phenomenon makes the Oregon coast significantly different from other upwelling regions (e.g., the equatorial Pacific or the northern Indian Ocean) that are sources of CO<sub>2</sub> to the atmosphere. *Hales et al.* [2004] also showed a seasonal (between May and August) increase in subsurface P<sub>CO2</sub> (due to respiration of settling particles). This respiration at depth and winter downwelling could mix this shelf derived carbon into the deep ocean interior.

[31] *Chase et al.* [2005] expanded their previous studies of iron distributions in Oregon coastal waters [*Chase et al.*, 2002] to study the seasonal progression of iron supply in coastal regions with varying topography. Iron is supplied by both fluvial inputs and upwelling of deep water with higher concentrations in spring than in summer and higher concentrations in the northern sites (45°N with steep topography) than in the south (44°N with less steep topography). *Chase et al.* [2005] also used moored sensors to measure the backscatter of particles and to evaluate the movement of particles across the shelf. The optical backscatter data was inconsistent with the notion of conveyor belt circulation of iron-bearing particles, and provide evidence for the sinking and down-slope transport of particles over the inner- and midshelf regions. In contrast to evidence of iron limitation and iron stress off the coast of California [*Hutchins and Bruland*, 1998], in the COAST region off Oregon availability of dissolved iron is sufficient to meet the demands of phytoplankton as shown by the complete drawdown of nitrate and silicate. Accumulation of dissolved iron in bottom water does occur over the upwelling season presumably as a result of remineralization of sinking particles.

[32] *Ruttenberg and Dyhrman* [2005] show that differences in the spatial and temporal patterns of phosphate are explained by patterns of upwelling and residence times as controlled by the shelf topography. During May 2001 the range in phosphate concentrations were similar along the northern shelf and over Heceta Bank, however, phytoplankton were only able to draw surface phosphate concentrations to low levels over the Bank. The surface water inorganic and organic phosphorus covary in opposing ways with temperature and chlorophyll suggesting a phytoplankton sink for inorganic P and a phytoplankton source for organic P. Enzyme activity and dissolved organic phosphorus were higher over the bank than along the northern shelf transect, supporting the notion that the net activity of phytoplankton was greater over the Bank. Results presented by *Ruttenberg and Dyhrman* [2005] clearly illustrate the dynamic range of nutrient distribution and phytoplankton activity in this coastal upwelling region and the differences in phosphorus utilization that appear to result from the different circulation patterns along the coast.

[33] Coastal upwelling is associated with rapid production and accumulation of organic material in both the particulate and dissolved form. *Karp-Boss et al.* [2004] examined the spatial and temporal variability of particulate organic material (POM) using high-resolution vertical pro-

filing of beam attenuation calibrated with discrete measurements of particulate carbon. The magnitude of short-term variations was the same order as that of seasonal variations reported previously [Small *et al.*, 1989]. High levels of particulate organic carbon (POC) showed a restriction to the inner shelf where the shelf is narrow and a much broader cross-shelf distribution over the Bank. Elevated concentrations of chlorophyll and POC were observed near the bottom and this material may be transported across the shelf via the benthic nepheloid layer.

[34] Wetz and Wheeler [2003] examined the production and partitioning of phytoplankton-derived organic matter in deck incubations. During exponential growth 80% of the total accumulated organic carbon was in particulate (POC) form. After nutrient (nitrate) depletion dissolved organic carbon and nitrogen were released. On the basis of measured concentrations of nitrate and accumulated total organic carbon, more carbon was fixed than predicted from Redfield ratios. The production of DOC after phytoplankton blooms appears to result from continuation of photosynthesis and release of carbon-rich carbohydrates. The long-term accumulation of DOC seasonally off the coast of Oregon is likely prevented by the dynamics of the alongshore and upwelling circulation [Smith, 1981]. Wetz and Wheeler [2004] further examined the response of bacterioplankton to phytoplankton-derived dissolved organic material. Coincident with nitrate depletion and accumulation of dissolved organic material, bacterial abundances and growth rates increased dramatically. Degradation of dissolved carbon was not complete suggesting that environmental controls inhibit bacteria populations and may allow export of the phytoplankton derived organic material from shelf.

### 3.8. Distribution and Characteristics of Biological Communities

[35] The phytoplankton community off the coast of Oregon during the upwelling season is often dominated by large chain-forming diatoms. During COAST, several studies characterized the phytoplankton communities present during May and August 2001. During May 2001, the three most abundant genera were *Thalassiosira* and *Thalassionema* (both chain-forming diatoms) and *Pseudo-nitzschia*, a 100- $\mu\text{m}$ -long coastal diatom [Ruttenberg and Dyrman, 2005]. Phytoplankton blooms during three August 2001 incubations were dominated by *Chaetoceros* sp. ( $>20 \mu\text{m}$  cells) and one was dominated by a small ( $12 \times 3 \mu\text{m}$ ) diatom *Leptocylindrus minimus* [Wetz and Wheeler, 2003]. The high relative abundance of diatoms in these coastal waters is also indicated by the simultaneous drawdown of silicate and nitrate in the water column [Chase *et al.*, 2005].

[36] Eisner and Cowles [2005] examine the spatial variations in phytoplankton characteristics by using in situ optics, pigment analysis and hydrographic measurements. High levels of chlorophyll in surface samples from inshore and midshelf stations also contain a high fraction of fucoxanthin, indicating a dominance of diatoms. High levels of photoprotective pigments can be an indicator of high-light and low-nutrient environments. The ratio of photoprotective to photosynthetic carotenoids off the coast of Oregon increases from onshore to offshore. The offshore increases in photoprotective carotenoids are correlated with

warmer, more nutrient-deplete water. Spatial patterns in optically derived parameters corresponded to water mass distributions: coastal upwelling regions with high nutrients and chlorophyll (predominantly diatoms) contrasted with Columbia river plume and offshore water with lower chlorophyll, fewer diatoms and greater relative abundances of prymnesiophytes and prokaryotes.

[37] Although the phytoplankton in shelf waters are dominated by diatoms, small phytoplankton and cyanobacteria are also present. Variations in the spectral beam attenuation measurements in surface waters also suggest a greater contribution by small particles to the particle size distribution for offshore compared with nearshore waters [Eisner and Cowles, 2005]. However, Sherr *et al.* [2004] found a consistent pattern of lowest abundances of small-sized phytoplankton in the shelf region despite high nutrient and chlorophyll concentrations. The abundance of the small cells increases seaward of the upwelling front. The distribution of phytoplankton suggests a dramatic shift in the structure of pelagic food webs from the shelf upwelling blooms dominated by diatoms to the slope and basin food webs dominated by small phytoplankton.

[38] Lamb and Peterson [2005] use a Multiple Opening Closing Net and Environmental Sensing System (MOCNESS) to study the vertical distribution of zooplankton alongshore and across the shelf off Oregon. The four dominant copepods were *Calanus marshallae*, *Pseudocalanus mimus*, *Acartia longiremis* and *Centrophages abdominalis* and the dominant euphausiid was *Euphausia pacifica*. As seen for the phytoplankton, the zooplankton were confined to shelf waters suggesting little loss of plankton to offshore waters by advection. They found naupliar and early copepodite stages of *C. marshallae* and *P. mimus* in the warm, phytoplankton-rich upper 20 m of water, while the older stages were found at progressively deeper strata. Similarly, euphausiid larvae were most abundant within the upper 20 m of water while adults and juveniles lived in deeper water. Since neither group was abundant beyond the shelf break, cross-shelf losses appear to be small. On the basis of modeling results and physical oceanographic observations, Lamb and Peterson [2005] suggest that phytoplankton and zooplankton are retained within the study region because of a recirculating cyclonic circulation that often sets up on the Bank. However, it appears that when upwelling winds are strong, water and plankton are lost from the southern end of the Bank due to jet separation. Observations on the Bank are in contrast to observations made during the GLOBEC program south of Heceta Bank, near Cape Blanco and off northern California mesoscale eddies, where jets and filaments transport significant quantities of zooplankton into offshore oceanic waters.

[39] Sutor *et al.* [2005] use an acoustical approach to assess zooplankton distributions and found steep, fine-scale vertical gradients in acoustic backscatter over the shelf, with 10–15 dB changes in 265 and 420 kHz backscatter occurring over vertical intervals of 1–2 m. They show that two different acoustical sampling systems yield similar patterns in acoustical backscatter, provided that each system is operating well above its detection threshold. Using a TAPS acoustics system mounted on the MOCNESS frame, Sutor *et al.* [2005] found that steep gradients in acoustic backscatter were usually inadequately sampled by the

MOCNESS, complicating calibration of acoustic estimates with direct net collections of zooplankton.

### 3.9. Ecosystem Modeling

[40] A nutrient-phytoplankton-zooplankton-detritus (NPZD) numerical model has been used to study the ecosystem response to upwelling in the COAST region. A two-dimensional version [Newberger *et al.*, 2003; Spitz *et al.*, 2003] shows that the mean phytoplankton concentration is maximum onshore of the upwelling jet while the mean zooplankton concentration is highest farther offshore, the latter a robust result even when varying a large number of NPZD model parameters (e.g., zooplankton grazing rate increased, detritus sinking rate decreased). These distributions are consistent with previous observational studies [Small and Menzies, 1981]. The wind variability and the parameter values have little effect on the mean primary productivity, but have a larger effect on the fraction of primary productivity that is supported by new nitrogen (i.e., the  $f$  ratio) [Spitz *et al.*, 2003]. Studies coupling the NPZD models to three-dimensional coastal circulation models off central Oregon show that even for a narrow shelf region (e.g., north of Newport), the two- and three-dimensional (3-D) simulated phyto- and zooplankton concentrations display different offshore patterns and amplitudes [Spitz *et al.*, 2005]. The 3D model results show that the largest mean chlorophyll concentrations are located inshore of the coastal jet along the entire coast, while the highest zooplankton concentrations are offshore of the jet except over Heceta Bank. Spitz *et al.* [2005] evaluate the balance between physical and biological forcing in controlling the cross-shelf patterns of distribution of nutrients, phytoplankton and zooplankton for portions of the coast with varying topography. They show that during downwelling phytoplankton stocks are controlled by grazing while zooplankton stocks are controlled by physical forcing. During upwelling, physical forcing leads to low-standing stocks of phytoplankton and zooplankton nearshore, while farther offshore biological forcing (high nutrient availability, high phytoplankton growth rates out competing grazing rates) dominates. Spitz *et al.* [2005] also show that 20 day intraseasonal oscillations [Bane *et al.*, 2005] are also apparent in the modeled phyto- and zooplankton fields during summer 2001.

## 4. Summary and Future Research

[41] Through intensive measurements of the coastal ocean and atmosphere, and significant advances in techniques for ocean and ecosystem modeling, the COAST program has provided new understanding of coastal upwelling. Coordinated use of observations and models show how currents interact with the seafloor to create areas of concentrated phytoplankton production off the coast of Oregon. While this production fuels a successful fishery in the region, the eventual decay of phytoplankton leads to hypoxia (low levels of oxygen) in bottom waters that may impact nearshore fish and invertebrate communities. COAST researchers have also shown that absorption of carbon dioxide by phytoplankton makes the central Oregon shelf a net sink for atmospheric carbon dioxide. If this result can be extrapolated to large portions of the continental shelf off the west coast of the U.S., it will represent a major

fraction of the carbon sink for the entire North Pacific and provide additional insight on the global carbon cycle as a whole.

[42] COAST researchers are currently analyzing data sets and conducting modeling focused on a January–February 2003 wintertime experiment. Little research has been done on wintertime circulation and the resulting ecosystem response off the U.S. west coast. Results will provide a sharp contrast to those reported here for summertime upwelling. Remaining research includes quantifying the transport of biogeochemically important material off the continental shelf in association with the flow-topography interaction over Heceta Bank. Circulation and ecosystem models will continue to be used to test existing and new research hypotheses for coastal ocean processes, including the influence of physical processes versus biological processes in the formation and impact of hypoxic waters.

[43] **Acknowledgments.** We thank John Klinck and other members of the *JGR-Oceans* staff for their help in editing and shepherding this special section to completion. Special section editors Ed Dever (formerly Scripps Institution of Oceanography, now at OSU) and Hans Dam (University of Connecticut) did an excellent job in reviewing the papers. Thanks to our COAST coinvestigators for their many suggestions for improving this overview. We acknowledge the outstanding contributions of the many technicians, ship personnel, postdoctoral research associates, and students who helped make this interdisciplinary project a success. The COAST program was supported by the National Science Foundation's (NSF) Coastal Ocean Process (CoOP) program, and we thank Larry Clark and Alexandra Isern for their tireless support and especially for their efforts to help arrange the multiship field studies conducted in summer 2001. This research was primarily supported by NSF grant OCE-9907854, with additional support by NSF grants OCE-9907919, OCE-9907953, and OCE-0119134.

## References

- Bane, J. M., M. D. Levine, R. M. Samelson, S. M. Haines, M. F. Meaux, N. Perlin, P. M. Kosro, and T. Boyd (2005), Atmospheric forcing of the Oregon coastal ocean during the 2001 upwelling season, *J. Geophys. Res.*, doi:10.1029/2004JC002653, in press.
- Barnes, C. A., A. C. Duxbury, and B. A. Morse (1972), Circulation and selected properties of the Columbia River effluent at sea, in *The Columbia River Estuary and Adjacent Ocean Waters*, edited by A. T. Pruter and D. A. Alverson, pp. 41–80, Univ. of Wash. Press, Seattle.
- Barth, J. A., S. D. Pierce, and R. L. Smith (2000), A separating coastal upwelling jet at Cape Blanco, Oregon and its connection to the California Current System, *Deep Sea Res., Part II*, 47, 783–810.
- Barth, J. A., S. D. Pierce, and R. M. Castelao (2005a), Time-dependent, wind-driven flow over a shallow midshelf submarine bank, *J. Geophys. Res.*, doi:10.1029/2004JC002761, in press.
- Barth, J. A., S. D. Pierce, and T. J. Cowles (2005b), Mesoscale structure and its seasonal evolution in the northern California Current system, *Deep Sea Res., Part II*, 52, 5–28.
- Batchelder, H. P., et al. (2002), The GLOBEC Northeast Pacific California Current System program, *Oceanography*, 15, 36–47.
- Boyd, T., M. D. Levine, P. M. Kosro, S. R. Gard, and W. Waldorf (2002), Observations from moorings on the Oregon continental shelf (May–August 2001), *Data Rep. 190, Ref. 2002-6*, Coll. of Oceanic and Atmos. Sci., Ore. State Univ., Corvallis.
- Buttman, B., R. C. Beardsley, B. Magnell, D. Frye, J. A. Vermersch, R. Schlitz, R. Limeburner, W. R. Wright, and M. A. Noble (1982), Recent observations of the mean circulation on Georges Bank, *J. Phys. Oceanogr.*, 12, 569–591.
- Castelao, R. M., and J. A. Barth (2005), Coastal ocean response to summer upwelling favorable winds in a region of alongshore bottom topography variations off Oregon, *J. Geophys. Res.*, 110, C10S04, doi:10.1029/2004JC002409.
- Chase, Z., A. van Geen, P. M. Kosro, J. Marra, and P. A. Wheeler (2002), Iron, nutrient, and phytoplankton distributions in Oregon coastal waters, *J. Geophys. Res.*, 107(C10), 3174, doi:10.1029/2001JC000987.
- Chase, Z., B. Hales, T. Cowles, R. Schwartz, and A. van Geen (2005), Distribution and variability of iron input to Oregon coastal waters during the upwelling season, *J. Geophys. Res.*, 110, C10S12, doi:10.1029/2004JC002590.

- Corwith, H. L., and P. A. Wheeler (2002), El Nino related variations in nutrient and chlorophyll distributions off Oregon, *Prog. Oceanogr.*, *54*, 361–380.
- Dugdale, R. C., and F. P. Wilkerson (1989), New production in the upwelling center off Point Conception, California: Temporal and spatial patterns, *Deep Sea Res.*, *36*, 985–1007.
- Eisner, L., and T. J. Cowles (2005), Spatial variations in phytoplankton pigment ratios, optical properties, and environmental gradients in Oregon coast surface waters, *J. Geophys. Res.*, *110*, C10S14, doi:10.1029/2004JC002614.
- Erofeeva, S. Y., G. D. Egbert, and P. M. Kosro (2003), Tidal currents on the central Oregon shelf: Models, data and assimilation, *J. Geophys. Res.*, *108*(C5), 3148, doi:10.1029/2002JC001615.
- Feinberg, L. R., and W. T. Peterson (2003), Variability in duration and intensity of euphausiid spawning off central Oregon, 1996–2001, *Prog. Oceanogr.*, *57*, 363–379.
- Gan, J., and J. S. Allen (2005), Modeling upwelling processes off the Oregon coast during summer 2001, *J. Geophys. Res.*, *110*, C10S07, doi:10.1029/2004JC002692.
- Grantham, B. A., F. Chan, K. J. Nielsen, D. S. Fox, J. A. Barth, A. Huyer, J. Lubchenco, and B. A. Menge (2004), Upwelling-driven nearshore hypoxia signals ecosystem and oceanographic changes in the northeast Pacific, *Nature*, *429*, 749–754.
- Hales, B., T. Takahashi, and L. Bandstra (2004), Atmospheric CO<sub>2</sub> uptake by a coastal upwelling system, *Global Biogeochem. Cycles*, *19*, GB1009, doi:10.1029/2004GB002295.
- Hales, B., J. N. Moum, P. A. Covert, and A. Perlin (2005), Irreversible nitrate fluxes due to turbulent mixing in a coastal upwelling system, *J. Geophys. Res.*, *110*, C10S11, doi:10.1029/2004JC002685.
- Halpern, D. (1976), Structure of a coastal upwelling event observed off Oregon during July 1973, *Deep Sea Res.*, *23*, 495–508.
- Hickey, B. M. (1997), The response of a steep-sided, narrow canyon to time-variable wind forcing, *J. Phys. Oceanogr.*, *27*, 697–726.
- Hill, J. K., and P. A. Wheeler (2002), Organic carbon and nitrogen in the northern California current system: Comparison of offshore, river plume and coastally upwelled water, *Prog. Oceanogr.*, *53*, 369–387.
- Hutchins, D. A., and K. W. Bruland (1998), Iron-limited diatom growth and Si:N uptake ratios in a coastal upwelling regime, *Nature*, *393*, 561–564.
- Huyer, A., R. L. Smith, and E. J. Sobey (1978), Seasonal differences in low-frequency current fluctuations over the Oregon continental shelf, *J. Geophys. Res.*, *83*, 5077–5089.
- Huyer, A., E. Sobey, and R. Smith (1979), The spring transition in currents over the Oregon continental shelf, *J. Geophys. Res.*, *84*, 6995–7011.
- Karp-Boss, L., P. A. Wheeler, B. Hales, and P. Covert (2004), Distributions and variability of particulate organic matter in a coastal upwelling system, *J. Geophys. Res.*, *109*(C9), C09010, doi:10.1029/2003JC002184.
- Keister, J. E., and W. T. Peterson (2003), Zonal and seasonal variations in zooplankton community structure off the central Oregon coast, 1998–2000, *Prog. Oceanogr.*, *57*, 341–361.
- Kirincich, A. R., J. A. Barth, B. A. Grantham, B. A. Menge, and J. Lubchenco (2005), Wind-driven inner-shelf circulation off central Oregon during summer, *J. Geophys. Res.*, *110*, C10S03, doi:10.1029/2004JC002611.
- Kosro, P. M. (2005), On the spatial structure of coastal circulation off Newport, Oregon, during spring and summer 2001, in a region of varying shelf width, *J. Geophys. Res.*, doi:10.1029/2004JC002769, in press.
- Kundu, P. K., and J. S. Allen (1976), Some three-dimensional characteristics of low-frequency current fluctuations near the Oregon coast, *J. Phys. Oceanogr.*, *6*, 181–199.
- Kurapov, A. L., G. D. Egbert, J. S. Allen, and R. N. Miller (2003), M<sub>2</sub> internal tide off Oregon: Inferences from data assimilation, *J. Phys. Oceanogr.*, *33*, 1733–1757.
- Kurapov, A. L., J. S. Allen, G. D. Egbert, R. N. Miller, P. M. Kosro, M. Levine, and T. Boyd (2005a), Distant effect of assimilation of moored currents into a model of coastal wind-driven circulation off Oregon, *J. Geophys. Res.*, *110*, C02022, doi:10.1029/2003JC002195.
- Kurapov, A. L., J. S. Allen, G. D. Egbert, R. N. Miller, P. M. Kosro, M. D. Levine, T. Boyd, and J. A. Barth (2005b), Assimilation of moored velocity data in a model of coastal wind-driven circulation off Oregon: Multivariate capabilities, *J. Geophys. Res.*, *110*, C10S08, doi:10.1029/2004JC002493.
- Kurapov, A. L., G. D. Egbert, J. S. Allen, and R. N. Miller (2005c), Modeling bottom mixed layer variability on the mid-Oregon shelf during summer, *J. Phys. Oceanogr.*, in press.
- Lamb, J., and W. Peterson (2005), Ecological zonation of zooplankton in the COAST study region off central Oregon in June and August 2001 with consideration of retention mechanisms, *J. Geophys. Res.*, *110*, C10S15, doi:10.1029/2004JC002520.
- Lentz, S. J. (1992), The surface boundary layer in coastal upwelling systems, *J. Phys. Oceanogr.*, *22*, 1517–1539.
- Lentz, S. J., and D. C. Chapman (2004), The importance of nonlinear cross-shelf momentum flux during wind-driven coastal upwelling, *J. Phys. Oceanogr.*, *34*, 2444–2457.
- Mooers, C. N. K., C. A. Collins, and R. L. Smith (1976), The dynamic structure of the frontal zone in the coastal upwelling region off Oregon, *J. Phys. Oceanogr.*, *6*, 3–21.
- Morgan, C. A., W. T. Peterson, and R. L. Emmett (2003), Onshore-offshore variations in copepod community structure off the Oregon coast during the summer upwelling season, *Mar. Ecol. Prog. Ser.*, *249*, 223–236.
- Moum, J. N., and J. D. Nash (2000), Topographically induced drag and mixing at a small bank on the continental shelf, *J. Phys. Oceanogr.*, *30*, 2049–2054.
- Moum, J. N., A. Perlin, J. M. Klymak, M. D. Levine, T. Boyd, and P. M. Kosro (2004), Convectively-driven mixing in the bottom boundary layer, *J. Phys. Oceanogr.*, *34*, 2189–2202.
- Newberger, P. A., J. S. Allen, and Y. H. Spitz (2003), Analysis and comparison of three ecosystem models, *J. Geophys. Res.*, *108*(C3), 3061, doi:10.1029/2001JC001182.
- Oke, P. R., J. S. Allen, R. N. Miller, G. D. Egbert, and P. M. Kosro (2002a), Assimilation of surface velocity data into a primitive equation coastal ocean model, *J. Geophys. Res.*, *107*(C9), 3122, doi:10.1029/2000JC000511.
- Oke, P. R., J. S. Allen, R. N. Miller, G. D. Egbert, J. A. Austin, J. A. Barth, T. J. Boyd, P. M. Kosro, and M. D. Levine (2002b), A modeling study of the three-dimensional continental shelf circulation off Oregon. Part I: Model-data comparisons, *J. Phys. Oceanogr.*, *32*, 1360–1382.
- Oke, P. R., J. S. Allen, R. N. Miller, and G. D. Egbert (2002c), A modeling study of the three-dimensional continental shelf circulation off Oregon. Part II: Dynamical analysis, *J. Phys. Oceanogr.*, *32*, 1383–1403.
- Ott, M. W., J. A. Barth, and A. Y. Erofeev (2003), Microstructure measurements of a summer downwelling front, *Eos Trans. AGU*, *84*(46), Ocean Meet. Suppl., Abstract OS42M-07.
- Ott, M. W., J. A. Barth, and A. Y. Erofeev (2004), Microstructure measurements from a towed undulating platform, *J. Atmos. Oceanic Technol.*, *21*, 1621–1632.
- Pearcy, W. G., D. L. Stein, M. A. Hixon, E. K. Pikitch, W. H. Barss, and R. M. Starr (1989), Submersible observations of deep-reef fishes of Heceta Bank, *Oregon Fish. Bull.*, *87*, 955–965.
- Perlin, N., R. M. Samelson, and D. B. Chelton (2004), Scatterometer and model wind and wind stress in the Oregon-California coastal zone, *Mon. Weather Rev.*, *132*, 2110–2129.
- Perlin, A., J. N. Moum, and J. M. Klymak (2005a), Response of the bottom boundary layer over a sloping shelf to variations in alongshore wind, *J. Geophys. Res.*, *110*, C10S09, doi:10.1029/2004JC002500.
- Perlin, A., J. N. Moum, J. M. Klymak, M. D. Levine, T. Boyd, and P. M. Kosro (2005b), A modified law-of-the-wall applied to oceanic bottom boundary layers, *J. Geophys. Res.*, *110*, C10S10, doi:10.1029/2004JC002310.
- Peterson, W. T., C. B. Miller, and A. Hutchinson (1979), Zonation and maintenance of copepod populations in the Oregon upwelling zone, *Deep Sea Res.*, *Part A*, *26*, 467–494.
- Ruttenberg, K. C., and S. T. Dyrman (2005), Temporal and spatial variability of dissolved organic and inorganic phosphorous, and metrics of phosphorous bioavailability in an upwelling-dominated coastal system, *J. Geophys. Res.*, doi:10.1029/2004JC002837, in press.
- Samelson, R., P. Barbour, J. Barth, S. Bielli, T. Boyd, D. Chelton, P. Kosro, M. Levine, E. Skillingstad, and J. Wilczak (2002), Wind stress forcing of the Oregon coastal ocean during the 1999 upwelling season, *J. Geophys. Res.*, *107*(C5), 3034, doi:10.1029/2001JC000900.
- Sherr, E. B., B. F. Sherr, and P. A. Wheeler (2004), Distribution of coccoid cyanobacteria and small eukaryotic phytoplankton in the upwelling system off the Oregon coast during 2001 and 2002, *Deep Sea Res.*, *Part II*, *52*, doi:10.1016/j.dsr2.2004.09.020.
- Small, L. F., and D. W. Menzies (1981), Patterns of primary productivity and biomass in a coastal upwelling region, *Deep Sea Res.*, *Part A*, *28*, 123–149.
- Small, L. F., H. Pak, D. M. Nelson, and C. S. Weimer (1989), Seasonal dynamics of suspended particulate matter, in *Coastal Oceanography of Washington and Oregon*, edited by M. R. Landry and B. M. Hickey, pp. 255–285, Elsevier, New York.
- Smiles, M. C., and W. G. Pearcy (1970), Size structure and growth rate of *Euphausia pacifica* off the Oregon coast, *Fish. Bull.*, *69*, 79–86.
- Smith, R. L. (1981), A comparison of the structure and variability of the flow field in three coastal upwelling regions: Oregon, northwest Africa, and Peru, in *Coastal Upwelling, Coastal Estuarine Ser.*, vol. 1, edited by F. A. Richards, pp. 107–118, AGU, Washington, D. C.
- Spitz, Y. H., P. A. Newberger, and J. S. Allen (2003), Ecosystem response to upwelling off the Oregon coast: Behavior of three nitrogen-based models, *J. Geophys. Res.*, *108*(C3), 3062, doi:10.1029/2001JC001181.

- Spitz, Y. H., J. S. Allen, and J. Gan (2005), Modeling of ecosystem processes on the Oregon shelf during the 2001 summer upwelling, *J. Geophys. Res.*, *110*, C10S17, doi:10.1029/2005JC002870.
- Sutor, M., T. J. Cowles, W. T. Peterson, and J. Lamb (2005), Comparison of acoustic and net sampling systems to determine patterns in zooplankton distribution, *J. Geophys. Res.*, *110*, C10S16, doi:10.1029/2004JC002681.
- Torgimson, G. M., and B. M. Hickey (1979), Barotropic and baroclinic tides over the continental slope and shelf off Oregon, *J. Phys. Oceanogr.*, *9*, 945–961.
- Trowbridge, J. H., and S. J. Lentz (1991), Asymmetric behavior of an oceanic boundary layer above a sloping bottom, *J. Phys. Oceanogr.*, *21*, 1171–1185.
- Trowbridge, J. H., and S. J. Lentz (1998), Dynamics of the bottom boundary layer on the northern California shelf, *J. Phys. Oceanogr.*, *28*, 2075–2093.
- van Geen, A., R. K. Takesue, J. Goddard, T. Takahashi, J. A. Barth, and R. L. Smith (2000), Carbon and nutrient dynamics during the coastal upwelling off Cape Blanco, Oregon, *Deep Sea Res., Part II*, *47*, 975–1002.
- Wetz, M. S., and P. A. Wheeler (2003), Production and partitioning of organic matter during simulated phytoplankton blooms, *Limnol. Oceanogr.*, *48*, 1808–1817.
- Wetz, M. S., and P. A. Wheeler (2004), Response of bacteria to simulated upwelling phytoplankton blooms, *Mar. Ecol. Prog. Ser.*, *272*, 49–57.
- Wroblewski, J. S. (1977), A model of phytoplankton plume formation during variable Oregon upwelling, *J. Mar. Res.*, *35*, 357–394.
- Wroblewski, J. S. (1980), A simulation of the distribution of *Acarta clausi* during Oregon upwelling, August 1973, *J. Plankton Res.*, *2*, 43–68.
- Wroblewski, J. S. (1982), Interaction of currents and vertical migration in maintaining *Calanus marshallae* in the Oregon upwelling zone—A simulation, *Deep Sea Res.*, *29*, 665–686.

---

J. A. Barth and P. A. Wheeler, College of Oceanic and Atmospheric Sciences, Oregon State University, 104 COAS Admin Building, Corvallis, OR 97331-5503, USA. (barth@coas.oregonstate.edu)